Indonesian Journal of Electrical Engineering and Computer Science
Vol. 11, No. 3, September 2018, pp. 1083~1093
ISSN: 2502-4752, DOI: 10.11591/ijeecs.v11.i3.pp1083-1093

Automated Detection of Microaneurysms using Probabilistic Cascaded Neural Network

Jeyapriya J, Umadevi K S, Jagadeesh Kannan R
School of Computing Science & Engineering, Vellore Institute of Technology, India

Article Info

Article history:

Received May 1, 2018
Revised Jun 21, 2018
Accepted Jun 28, 2018

Keywords:

Blood vessel
Detection of diabetic retinopathy
Retinal nerve hemorrhages
microaneurysms

ABSTRACT

The diagnosing features for Diabetic Retinopathy (DR) comprises of features occurring in and around the regions of blood vessel zone which will result into exudes, hemorrhages, microaneurysms and generation of textures on the albumen region of eye balls. In this study we presenta probabilistic convolution neural network based algorithms, utilized for the extraction of such features from the retinal images of patient's eyeballs. The classificat ions proficiency of various DR systems is tabulated and examined. The majority of the reported systems are profoundly advanced regarding the analyzed fundus images is catching up to the human ophthalmologist's characterization capacities.

Corresponding Author:

Jeyapriya J,
School of Computing Science & Engineering,
Vellore Institute of Technology, India.
Email: priyacseme@gmail.com

1. INTRODUCTION

Rapid advancement of diabetes has been the most prominent fundamental difficulties of availing proper health protection service. The measure of individuals influenced with the disease keeps on developing at a disturbing rate. The WHO (World Health Organization) expects the quantity of individuals with diabetics to increment from more than 125 million to over 350 million throughout the following two decades [1]. The circumstance is exacerbated by the way that one and only 50% of the patients know about there progression of disease. What's more, worsens the situation is as therapeutically, diabetes prompts to cause extreme complications as it progresses further. These intricacies incorporate large scale and smaller scale vascular changes which result in coronary illness, renal issues and retinopathy. For instance, survey in the USA alone demonstrate that diabetes is considered to the 5^{th} most deadliest disease, and till now there is no cure [2]. Diabetic retinopathy (DR) as shown in Figure 1 is a typical afteraffect of diabetes. Undoubtedly, it is common to the point that it is the main source of visual deficiency in the working populace of western nations [3], [4]. The rate of diabetes is expanding at an alarming rate. Regrettably, most of the nations often unable to record DR cases and thus need fundamental recording strategies for registering DR cases [5].

Early discovery of DR is critical, in light of the fact that treatment strategies can derailed the advancement of the disease. Majority of treatment strategies depend on laser based methods. Laser photocoagulation closes up visual blood vessels, which adequately stops their spillage. The central laser treatment strategy diminishes retinal thickening [6]-[8]. This may counteract declining of retinal swelling. To be particular, this treatment lessens the danger of vision misfortune by half. For a little number of cases, with aggregate vision misfortune, change is conceivable [9].

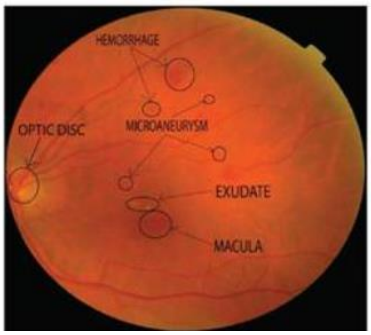

Figure 1. Illustration of different features involved in DR influenced retinal images

Analysis of retinal pictures is a growing research area that presently draws in bunches of enthusiasm from both researchers and doctors. The goal of this field is to create computational methods which will help measurement and representation of intriguing pathology and anatomical structures. These analysis framework works with advanced fundus images of the eye [10]. The strategy of taking fundus images begins by widening the pupil as shown in Figure 2 with pharmaceutical eye drops. After that the patient is requested to affix gaze with a specific end goal to record the retina in motionless position. While taking the photos, the patient will see a progression of repeated flashes. The whole procedure takes around five to ten minutes. To guarantee that DR treatment is performed on time, the eye fundus images of diabetic patients must be analyzed in any event once every year [11]. Include extraction techniques and examination Image handling can do both decrease the workload of screeners and assume a focal p art in quality affirmation undertakings. In this way, there has been an expansion in the use of computerized picture handling procedures for programmed identification of DR [12]. For instance, shading features on Bayesian measurable classifier were utilized to characterize every pixel into lesion or non -lesion classes [13]. The accompanying areas portray sets of retinal scenarios such as: haemorrhages, exudes, maculopathyand microaneurysms. Such identification procedures yield the majority of the features which are utilized as a part of computerized DR detection framework.

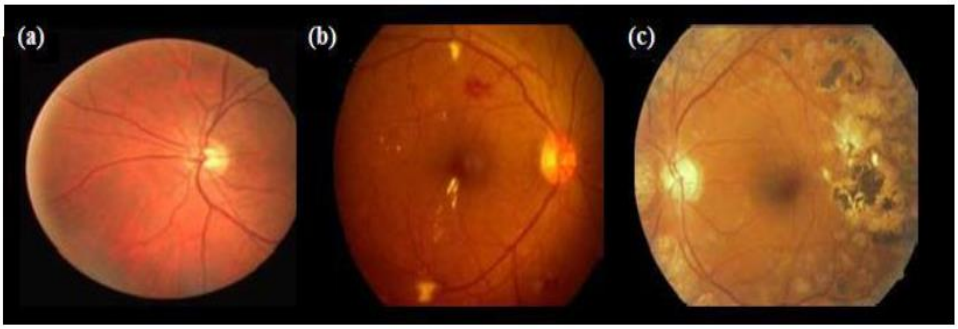

Figure 2. Sample DR influenced images for three stages i.e., (a) Normal, (b) Moderate, (c) Severe

Advanced fundus photography from the human eye gives clear images of the blood vessels in the retina. This technique gives a brilliant window to the record the true state of a patient's retina influenced by DR [14]. The blood vessel structure was extracted by subjecting the green part of the RGB fundus picture to various image processing algorithms [14]. Blood vessels were identified utilizing two -dimensional coordinated channels [15]. The Dark level profile of cross area of blood vessels that are been approximated by Gaussian filters. The idea of coordinated channel location of signals was utilized to recognize piece wise straight sections of blood vessels after the vessel classifier. Vessel focuses in a cross segment are found with a fuzzy-c-means classifier [16], [17]. This technique found and sketched out the boundaries of blood vessels in the given images by the utilization of a novel strategy to section blood vessels that compliments neighbourhood vessel properties with area based qualities of the retinal structure. The computer supported determination system been developed to help doctors in identifying irregularities connected with fundus

images of the retina [18]. Their proposed system can recog nize blood vessel convergences and it can distinguish precise widths in blood vessels. Electronic system for both extraction and quantitative depiction of the fundamental vascular symptomatic signs from fundus images in hypertensive retinopathy was exhibited [19]. The features they have considered are vessel tortuosity, summed up and central vessel narrowing, nearness of Gunn or Salus signs. Another system was proposed for the automated extraction of the vascular structure in retinal images, in view of a scanty following method was proposed [20]. Blood vessel focuses in a cross area are found by method for a fuzzy-c-means classifier. In the wake of following technique, the vessels distinguished fragments were associated in utilizing avaricious computation. A t last bifurcations and intersections were distinguished dissecting vessel end indicates with difference of the vessel structure. Blood vessel tracker calculation was created to decide the retinal vascular system is captured utilizing an advanced camera [21]. The tracker calculation identifies optic circle, lesions, for example, cotton fleeces spots, and fine nerve sores, for example, hemorrhages. This calculation recognizes supply routes and veins with an exactness of 78.4% and 66.5% separately [22].

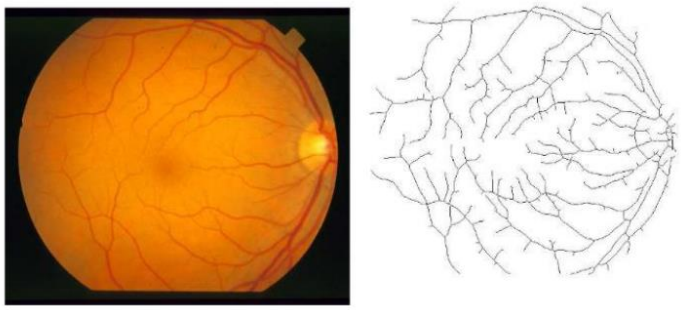

Figure 3. Results of retinal blood vessel detection

A strategy is been adopted for automated location and arrangement of vascular irregularities in diabetic retinopathy [23]. They recognized vascular variations from the norm utilizing scale and introduc tion particular Gabor channel banks. The proposed strategy orders retinal images as either gentle or serious cases in light of the Gabor channel yields. The microaneurysms in retinal fluorescienangiograms was recognized by first finding the fovea by sub-inspecting picture by figure of four every measurement [24]. Consequently, the picture was subjected to middle separating with a 5 by 5 veil to diminish high -recurrence segments. At that point the picture was related with a two-dimensional circularly symmetric triangular capacity with displayed net shading of the macula. Blood-vessel location as shown in Figure 3 calculation in view of the territorial recursive various leveled disintegration utilizing quadtrees and post-filtration of edges to concentrate blood vessels was considered [25]. This strategy could diminish bogus rejections of predominately huge edges and quicker in contrast with the current approach with lessened stockpiling prerequisites for the edge delineate. The work utilized the arteriolar-to-venular distance across proportion of retinal blood vessels as a pointer of disease related changes in the retinal blood vessel tree [26]. Their trial results show a 97.1% achievement rate in the recognizable proof of DR vessel beginning stages, and a 99.2% achievement rate in the following of retinal vessels. Another technique for surface based vessel division to beat this issue was proposed [27]. The Fuzzy CMeans (FCM) bunching calculation was utilized to order the component vectors into vessel or non -vessel in view of the surface properties. They contrasted their technique and handlabeled ground truth division for five images and accomplished 83.27% affectability and 99.62% specificity. The method divides the data into two parts, one is for learning, and another is for testing. For the purpose of identifying fundus images including the normal class or glaucoma set of classes. Application of support vector machines (SVM) was highly used is shown in Figure 6 [28], [29]. The determination of sign was made from the vertex coordinates based on the degrees of the different direction. The system was tested based on the percentage of success rate from the Harris point detection and availability for detecting sign on different range. The resulted one shown that not all Harris point in the was image detected although most of the images were possible in recognizing the sign direction of it [30]. A subpixel-accuracy edge detection algorithm was explored, based on the wavelet transformation with the cubic spline interpolation of the len's module appearance quality inspection system. It does firstly calculation of the maximum wavelet modulus, and detection of a pixel-accurate edge. Finally industrial measurement methods using this subpixel-accurate edge detection based algorithm was studied [31].

2. PROBLEM IDENTIFICATION

Microaneurysms recognition is imperative, on the grounds that these structures constitute the early conspicuous element of DR. The main reports which connect these structures to DR go back to 1879 [32], [33]. All the more as of late, it have analyzed the appearance and vanishing of microaneurysms in various periods of fluorescein angiography [34]. In a comparative study both arrangement rate and vanishing of microaneurysms in early DR were analyzed [35]. The microaneurysmsturnover were registered reliabibly from shading fundus images [36].

They utilized another strategy called MA-tracker to number microaneurysms as shown in Figure 4. They demonstrated that the microaneurysms stay stable after some time, however just 29% stay at a similar place. In illustration the green segment, of the RGB fundus picture, was gotten the microaneurysms. Like the exudates recognition calculation, first the conspicuous structures inside retina images, for example, blood vessel tree and optic plate are to be expelled. After that an advanced succession of picture preparing algorithms was utilized to decide the zones inside the fundus images to get microane urysms see in Figure 4 [37], [38]. The automated distinguishing features of diabetic retinopathy in view of the nearness of microaneurysms were considered [29]. The optometrists accomplished 97% affectability at 88% for every penny specificity and the mechanized retinopathy indicator accomplished 85% affectability at 90% specificity.

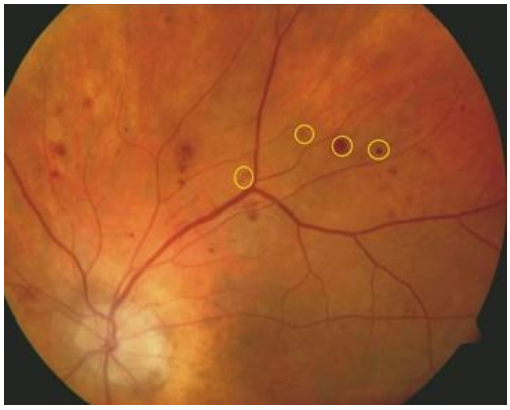

Figure 4. Results of microaneurysms detection

3. PROBABILISTIC CASCADED NEURAL NETWORK

Color features were utilized on Bayesian measurable classifier order every pixel into injury or non - sore classes. They have accomplished 100% exactness in distinguishing all the retinal images with exudates, and 70% precision in ordering typical retinal images as ordinary. DR and ordinary retina were grouped consequently utilizing picture preparing and multilayer perceptron neural system [39]. The system yielded an affectability of 80.21% and a specificity of 70.66%. Computerized analysis of NPDR, in light of three sores: hemorrhages and microaneurysmshard exudates, and cotton fleece spots, was concentrated on [40]. The technique could distinguish the NPDR arrange effectively with an exactness of 81.7%. The following steps represent the adopted methodlogy.

Step 1. Normalization

Normalization is employed to standardize the intensity values of an picture by adjusting the vary of its grey-level values in order that they lie among a desired vary of values e.g. zero mean and unit variance. Let I(i,j) denotes the gray-level value at picture element (i,j), M & VAR denote the calculable mean & variance of I(i,j) severally & N(i,j) de- notes the normalized gray-level value at picture element (i,j).

Algorithm: An algorithm for Normalization

Input: Input micro aneurysms image I(x, y), where x & y represents the pixel position.
Output: Segmented ridge region, I'(x, y).
Step1.1: Read Image I(x, y).
Step 1.2: Mask the Identifying Region M(x, y) from I(x, y).

Step 1.3: Break masked identified region into blocks b(m, n) × b(m,n).
Step 1.4: Find Intensity values$I(b(m,n),b(m,n))_{intensity}$ of the identified masked regional blocks.
Step 1.5: Evaluate Standard Deviation δ of intensity for each blocks $I(b(m,n),b(m,n))_{intensity}$.
Step 1.6: Repeat steps 1.5-1.6 &check:
if ($\delta < t$) **{**
I'(x,y) → V(x,y)
else
exit(0)
}
where,t is the threshold limit &*V(x,y)* is the vector indices location within the identified masked region.

Step 1.7: End Process.

Step 2. Image Orientation

Orientation of a micro-aneurysms is calculable by the smallest amount mean sq. orientation estimation algorithmic rule given by Hong during is shown in Figure 5 which foremost a block of size wXw (25X25) is centred at picture element (i, j) within the normalized micro-aneurysms image for every picture element during this block reckon, the Gaussian gradients x(i, j) and y(i, j) for each pixel position, that area unit the gradient magnitudes within the x & y directions severally.

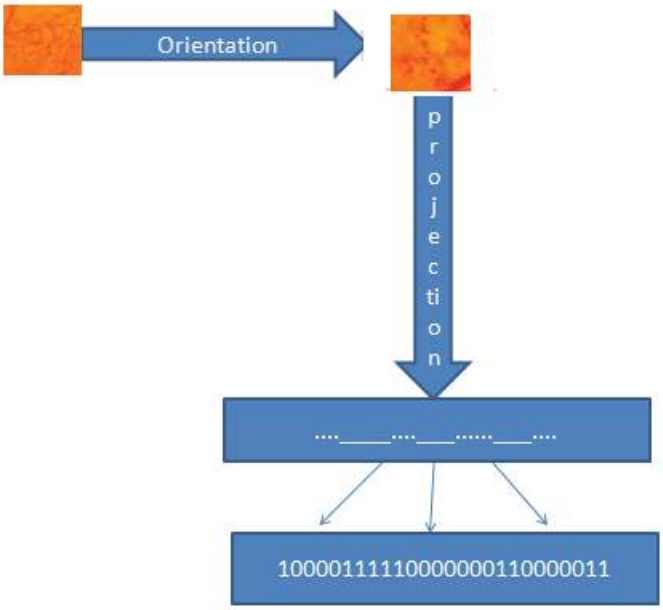

Figure 5. Orientation

Algorithm: An algorithm for Orientation

Input: Input normalized image I'(x, y), where x & y represents the pixel position, ridge location ($I(x,y)_{ridges}$), gradient deviation σ, σ' block gradient &σ_o orientation gradient
Output: Direction of the ridges, θ angle, + (i.e., 1) and –ve (i.e., 0) represents the clockwise or clockwise direction of the ridges.
Step 2.1: Read Image I'(x, y).
Step 2.2: Determine Image gradient σ' block gradient &σ_o orientation gradient respectively from the given gradient deviation:

σ' →Derivative of Gaussianused to compute image gradients.
σ_o →Derivative of GaussianSigma to smooththe final orientation vector field (v')

Step 2.3: Check for *l* =no. of. ridge location $I(x,y)_{ridges}$:
for i:l
{

If ($\sigma' < \sigma_o$) {

return $\theta \rightarrow +$

else

return $\theta \rightarrow -ve$

}

End *for loop*

Step 2.4: *End Process.*

Step-3 Feature Extraction

After orientation image microaneurysms options (Ridge Density, Ridge breath, and natural depression width) calculable.

Ridge breath: Ridge breath (Width) R is outlined as thickness of a ridge it's computed by investigating the quantity of pixels between consecutive maxima points of projected image, variety of 0's between 2 clusters of 1's can offer ridge breath

e.g. 11110000001111
In on top of example, ridge breath (width) is 6 pixels.

Valley breath: -Valley breath (Width) V is outlined as thickness of valleys it's computed by investigating the quantity of pixels between consecutive minima points of projected image, variety of 1's between 2 clusters of 0's can offer natural depression breath.

e.g.00001111111000
In on top of example, natural depression breath is 7 pixels.

Ridge Density: Ridge Density is outlined as variety of ridges in a very given block.

e.g. 001111100011111011
Above string contains 3 ridges in a very block.Thus ridge density is 3.

In the process involving classification of microaneurysmss ridge breadth and white lines area unit calculated. Using the probablistic model, first we create a graph model for the feature sets. Let us suppose that a given graph network data comprises of b+1 number of vertices. Thus, it can be modelled with the help of a graph tree, which is given as: G: =(N,E); where N represents the sets of vertices i.e, N=1,...,N_n and E is the edge set with the cardinality is given as $|N| = E$.

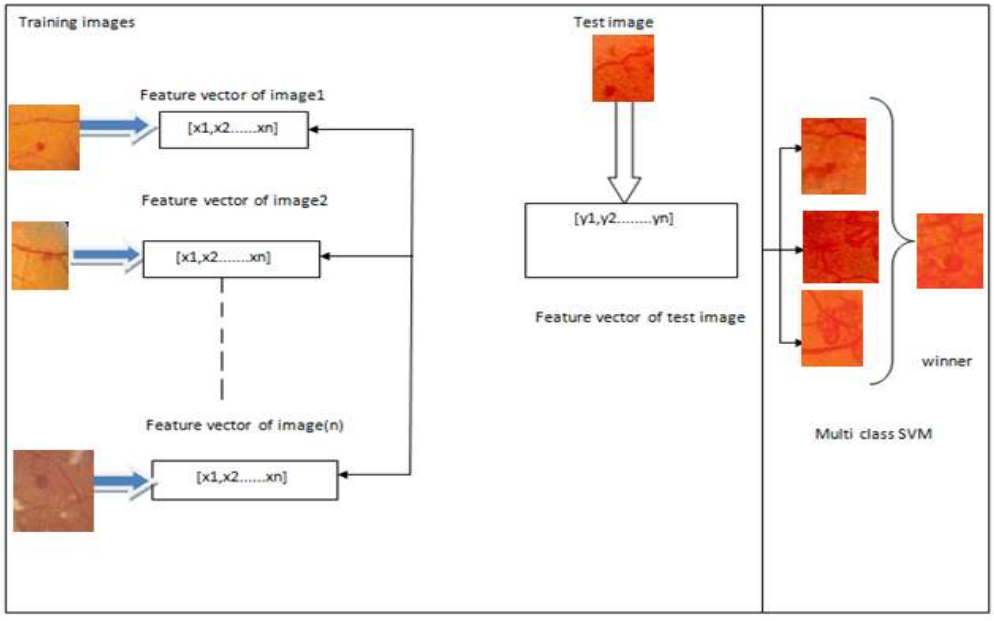

Figure 6. Multi class SVM

Here, each of the edges in form of the tree is rooted for index value n ruled by the probability flow from one edge to another and is derivable from source S to destination D with j amount of deviation in the form S_n+jD_n. Then the whole branch probability based graph flow model can be derived by initialising the conditional probability in form of a sequence traversed from parent to child nodes of two local posteriors i.e, probability of appearance of vertices (P_1) and that of edges (P_2) which is given by: $P_1 = (N^t|E_1^{1:t})$ & $P_2 = (N^t|E_2^{1:t})$. This is represented in the form of sequencized finite sets with multi object densities of $E_i^{1:t}$ observed edge sites. Here, the synchronization between such posterior is maintained as:

$$P_\alpha(N^D|E_1^{S:D}, E_2^{S:D}) = P_\alpha(N^D|E_1^{S:D} \cup E_2^{S:D})$$

Now, to overcome the problem of unknown correlation between no two distributions of independent variables the solution is:

$$P_\alpha(N^D|E_1^{S:D}, E_2^{S:D}) \propto \frac{P_\alpha(N^D|E_1^{S:D})P_\alpha(N^D|E_2^{S:D})}{P_\alpha(N^D|E_1^{S:D} \cup E_2^{S:D})}$$

Hence, the generalized posterior relationship can be represented in the form of geometric mean:

$$P_\alpha(N^D|E_1^{S:D}, E_2^{S:D}) = \frac{P_\alpha(N^D|E_1^{S:D})^{\alpha 1}P_\alpha(N^D|E_2^{S:D})^{\alpha 2}}{\int P_\alpha(N^D|E_1^{S:D})^{\alpha 1}P_\alpha(N^D|E_2^{S:D})^{\alpha 2}\delta N}$$

Where, $\alpha 1, \alpha 2$ $(\alpha 1 + \alpha 2 = 1)$ the parameters determining the relative probability of weighted distribution (w) between a specific hierarchical level of child and parent nodes. Now, in order to annonymize the percolated model of graph data, we need a rule set to algorithmically eliminate the sensitive vertices or add extra edges between labelled vertices to disrupt the probability of finding sensitive information. In this way we can induce anonymity in a quantitative way over the graph database.

Algorithm: Probabilistic CNN
Input: $\boldsymbol{m \times n}$ RGB standard Image
Where, m & n are the row & column of the given image.
Output: *CC, clustered features and Pixel location of microaneurysm images*
// for breaking down pixels into normalized illumination reflectance field

if $(\gamma_M \leq P_\alpha(N^D|E_1^{S:D}, E_2^{S:D}))$)
{
$$P_{nerve} = P(nerve|rg, N)$$

Else

$$P_{background} = (background|rg, \gamma_M)$$
}

*/ Where, M is the model of nerve color also embarked as low intensity pixels. γ_M&$\sum_M$ are mean & covariance of the pixel distribution based on intensities in *rg*color scheme after pre-processing. */

// Now, (x_1, y_1), (x_2, y_2), …,$(x_i, y_j) \in P_{nerve}$

while $l \leq \min\left(\sum_{i=1}^{N} D(v_i, n_i)\right)$ //D is the displacement vector

//Evaluate the feasible value of target nodes (pixels)T_{target}:

$$T_{target} = \sum_{i=1}^{N} D(x_i, y_i)$$

Create target vectors for feasible neighbouring nodes:

Loop: *for* 1 to n_i

$$\sum_{i=1}^{N} T(x_i, y_i) \leq R_{target}$$

//To create an associative CNN network of P_{nerve}

$$CC(i,j) = \sum_{i=1}^{m}\sum_{j=1}^{n} sgn(D(x_i, y_i) + \lambda T(x_i, y_i))$$

// λ is the lagrange multiplier.
end for loop
end while loop
END PROCESS

4. DISCUSSION

Exudates, hemorrhages, and microaneurysms were utilized for screening of DR subjects. The affectability and specificity of their product was 74.8% and 82.7%, separately in separating DR and typical subjects effectively. Early identification of DR (nearness of microaneurysms) was proposed in view of choice emotionally supportive network in many existing works. Bayes optimality criteria were utilized to distinguish microaneurysms. Their technique could distinguish the early phase of DR with an affectability of 100% and specificity of 67%. Ordinary, gentle, direct, extreme and productive DR stages is shown in Figure 2 were consequently characterized utilizing both zone and border of the RGB parts of the blood vessels together with a feedforward neural system. In the presented system with noisy images we achieved a normal arrangement proficiency over 84% and affectability, specificity were 90% and 100% individually. We have also utilized exudates and blood vessel range alongside surface parameters combined with neural system to order fundus images. We acquired a discovery precision of 93%, for non-noisy images with affectability and specificity of 90% and 100% individually. Figure 7 and 8 shows the average MSE and the factors influencing the recognition performances.

The specificity could be expanded similarly as 98.9%, however this expansion was joined by a fall in affectability to 90.8%. At a setting with 94.8% affectability and 52.8% specificity, no instances of sight undermining retinopathy were missed. It has researched both photography and optic plate geography method of the retinal thickness analyzer. Recognition of retinopathy was accomplished via automated steps evaluating with 90.5% affectability and 67.4% specificity when the probabilistic CNN used to estimate noisy coefficients as shown in Figure 9. Our work is based on the idea of the finding the topology of the features of a micro-aneurism in the given funds image & then coding it in logical sequence with the cascaded neural network.

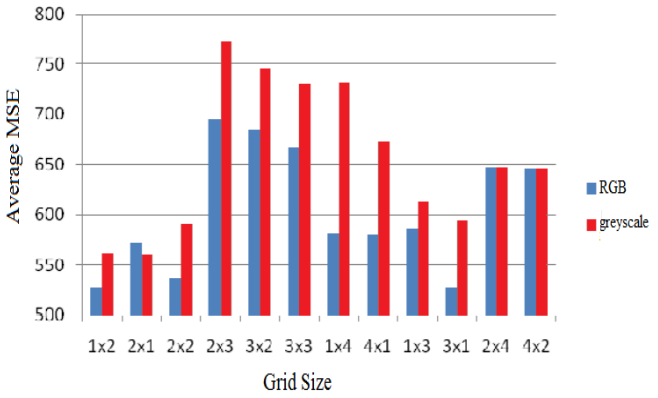

Figure 7. Average MSE across various Grid sizes for RGB & converted grey scale color space

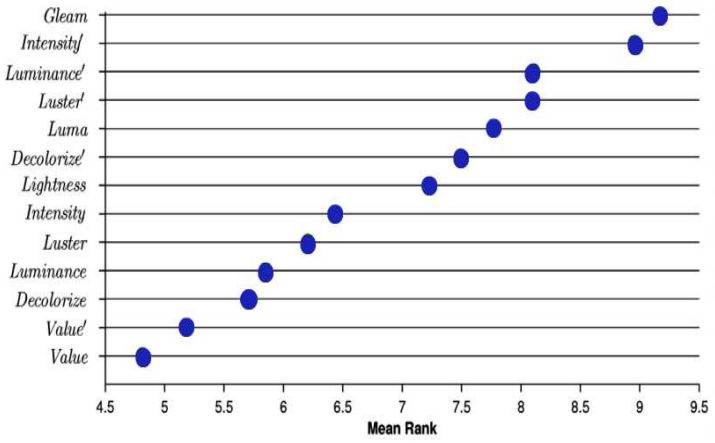

Figure 8. Aggregate Performance of method for pre-processing on the basis of perseverance of several qualities of the images in form of mean rank across datasets

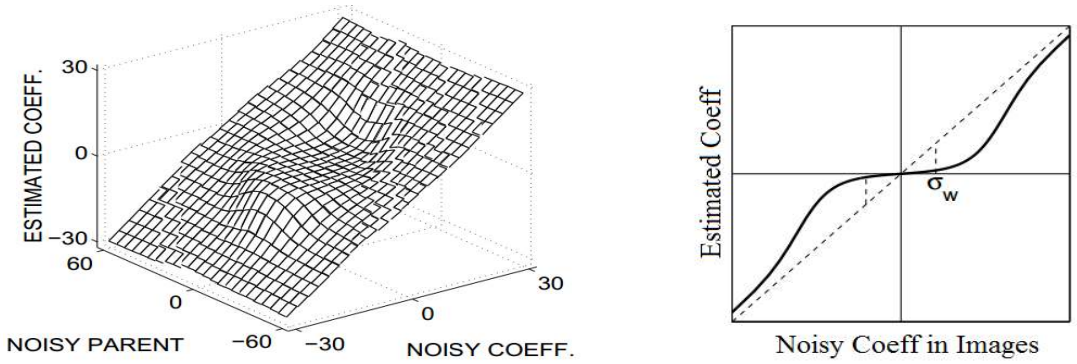

(a) (b)

Figure 9. Performance analysis of the CPRA MLPs (a) Plot For the evaluation of the estimated noisy coefficients (b) Estimatedcoefficients from probabilistic CNN and those of actual noisy coefficients in those Images

5. CONCLUSION

Extended period of diabetes prompts to DR, where the retina is harmed because of fluid spilling from the blood vessels. More often than that, the phase of DR is judged in light of blood vessels, exudes, hemorrhages, microaneurysms and surface. In this paper, we have examined distinctive techniques for features extraction and automatic techniques for icroaneurysms based on probabilistic CNN. As of late advances in imaging for DR screening allows top notch lasting records of the retinal features, which can be utilized for observing of diagnosis and prognosis for determining the course of treatment, and which can be checked on by an ophthalmologist, advanced images can possibly be handled via image processing based automated examination systems. A portion of the algorithms and systems investigated in this paper are near applicable for DR screening in clinical practice.

REFERENCES

[1] World Diabetes, A newsletter from the World Health Organization, 4, 1998.
[2] Cigna healthcare coverage position- A Report, 2007. Last accessed on 5th December 2007.
[3] Ong, G. L., Ripley, L. G., Newsom, R. S., Cooper, M., and Casswell, A. G., "Screening for sight-threatening diabetic retinopathy: comparison of fundus photography with automated color contrast threshold test", *Am. J. Ophthalmol.* vol. 137, no. 3, pp. 445–452, 2004.
[4] Hunter, A., Lowell, J., Owens, J., and Kennedy, L, "Quantification of diabetic retinopathy using neural networks and sensitivity analysis", *In Proceedings of Artificial Neural Networks in Medicine and Biology,* pp . 81-86, 2000.

[5] Kumar, A., "Diabetic blindness in India: the emerging scenario", *Indian J. Ophthalmol*, vol. 46, no. 2, pp. 65–66, 1998.
[6] Orbis. Last accessed December 2009.
[7] Watkins, J. P., "ABC of diabetes retinopathy ", *British Medical Journal* 326, pp. 924–926, 2003.
[8] Acharya, U. R., Lim, C. M., Ng, E. Y. K., Chee, C., and Tamura, T., "Computer-based detection of diabetes retinopathy stages using digital fundus images", *ProcInstMechEng* H. vol. 223, no. 5, pp . 545–553, 2009.
[9] Shahidi, M., Ogura, Y., Blair, N. P., and Zeimer, R., "Retinal thickness change after focal laser treatment of diabetic macular oedema", *Br J Ophthalmol*, vol. 78, no.11, pp. 827–830, 1994.
[10] Li, H., and Chutatape, O., "Fundus image feature extraction", *Proceedings 22nd Annual EMBS International Conference, Chicago*, pp. 3071-3073, 2000.
[11] Fong, D. S., Aiello, L., Gardner, T. W., King, G. L., Blankenship, G., Cavallerano, J. D., Ferris, F. L., and Klein, R., "Diabetic retinopathy ", *Diabetes Care v*ol. 26, no.1, pp . 226–229, 2003.
[12] Screening for Diabetic Retinopathy in Europe 15 years after the St. Vincent Declaration. *The Liverpool Declaration 2005*. Last accessed on 20th December 2007.
[13] Wang, H., Hsu, W., Goh, K. G., and Lee, M., "An effective approach to detect lesions in colour retinal images", *In Proceedings of the IEEE Conference on Computer Vision and Pattern Recognition*, pp. 181-187, 2000.
[14] Acharya, U. R., Lim, C. M., Ng, E. Y. K., Chee, C., and Tamura, T., "Computer based detection of diabetes retinopathy stages using digital fundus image", *J. Eng. Med.* vol. 223, no. H5, pp. 545–553, 2009.
[15] Chaudhuri, S., Chatterjee, S., Katz, N., Nelson, M., and Goldbaum, M., "Detection of blood vessels in retinal images using two-dimensional matched filters", *IEEE Trans. Med. Imag.* vol.8, no.3, pp. 263–269, 1989.
[16] Hoover, A. D., Kouzanetsova, V., and Goldbaum, M., "Locating blood vessels in retinal images by piecewise threshold probing of a matched filter response", *IEEE Trans. Med. Imag.* vol. 19, no. 3, pp. 203– 210, 2000.
[17] Sopharak, A., and Uyyanonvara, B., "Automatic exudates detection from diabetic retinopathy retinal image using fuzzy C-means and morphological methods", *Proceedings of the third IASTED international conference Advances in Computer Science and Technology,* Thailand, pp. 359-364, 2007.
[18] Fleming, D. A., Philip, S., Goatman, A. K., Williams, J. G., Olson, A. J., and Sharp, F. P., "Automated detection of exudates for diabetic retinopathy screening", *Phys. Med. Biol.* vol.52, no.24, pp . 7385– 7396, 2007.
[19] Hayashi, J., Kunieda, T., Cole, J., Soga, R., Hatanaka, Y., Lu, M., Hara, T., and Fujita, F., "A development of computer-aided diagnosis system using fundus images," *Proceeding of the 7th International Conference on Virtual Systems and MultiMedia (VSMM 2001),* pp. 429-438, 2001.
[20] Forracchia, M., Grisan, M. E., and Ruggeri, A., "Extraction and quantitative description of vessel features in hypertensive retinopathy fundus images", *Presented at CAFIA2001*, 2001.
[21] Grisan, I. E., Pesce, A., Giani, A., Foracchia, M., and Ruggeri, A., "A new tracking system for the robust extraction of retinal vessel structure", *26th Annual International Conference of the IEEE EMBS San Francisco, USA,* pp. 1620-1623, 2004.
[22] Zhang, X., and Chutatape, O., "Detection and classification of bright lesions in colour fundus images", *Int. Conf. on Image Processing* vol. 1, pp. 139–142, 2004.
[23] Vallabha, D., Dorairaj, R., Namuduri, K., and Thompson, H., "Automated detection and classification of vascular abnormalities in diabetic retinopathy", *Proceedings of 13th IEEE Signals, Systems and Computers,* vol. 2, pp. 1625-1629, 2004.
[24] Cree, J. M., Leandro, J. J. G., Soares, J. V. B., Cesar, R. M . Jr., Jelinek, H. F., and Cornforth, D., "Comparison of various methods to delineate blood vessels in retinal images", *Proceedings of the 16th Australian Institute of Physics Congress, Canberra*, 2005.
[25] Kandiraju, N., Dua, S., and Thompson, H. W., "Design and implementation of a unique blood vessel detection algorithm towards early diagnosis of diabetic retinopathy", *Proceedings of the International Conference on Information Technology: Coding and Computing (ITCC'05) IEEE Computer Society*, pp. 26- 31, 2005.
[26] Li, H., Hsu, W., Lee, M. L., and Wong, T. Y., "Automated grading of retinal vessel caliber", *IEEE Trans. Biomed. Eng. 52*, pp. 1352–1355, 2005.
[27] Bhuiyan, A., Nath, B., Chua, J., and Kotagiri, R., "Blood vessel segmentation from color retinal images using unsupervised texture classification", *IEEE Int. Conf. Image Processing, ICIP 5*, pp. 521–524, 2007.
[28] Osareh, A., M irmehdi, M ., Thomas, B., and M arkham, R., "Comparative exudate classification using support vector machines and neural networks", *The 5th International Conf. on Medical Image Computing and Computer-Assisted Intervention,* pp . 413-420, 2002.
[29] Anindita, S., Hamdani, Dyna, M. K., "The Contour Extraction of Cup in Fundus Images for Glaucoma Detection", *International Journal of Electrical and Computer Engineering (IJECE),* vol.6, no.6, pp .2797-2804, 2016.
[30] Hairol, N. M. S., M ohd, Z. A. R., Zalina, K., M ohd, S. M. A., Nursabillilah, M. A., Faizil, W., Tengku, M. M. T. A., "Sign Detection Vision Based M obile Robot Platform ", *Indonesian Journal of Electrical Engineering and Computer Science (IJEECS),* vol. 7, no. 2, pp . 524 - 532, 2017.
[31] Zhang, J. Z., He, Y., "A New M ethod for Appearance Quality Detection of Lens M odule Based on M achine Vision", *TELKOMNIKA (Telecommunication Computing Electronics and Control) Vol.14, No.2A, pp. 343-350, June 2016.*
[32] Walter, T., M assin, P., Erginay, A., Ordonez, R., Jeulin, C., and Klein, J. C., "Automatic detection of microaneurysms in color fundus images", *Med. Image Anal.* vol. 11, no. 6, pp. 555–566, 2007.
[33] Hellstedt, T., and Immonen, I., "Disappearance and formation rates of microaneurysms in early diabetic retinopathy", *Br. J. Ophthalmol*. vol. 80, no. 2, pp. 135–139, 1996.

[34] Jalli, P. Y., Hellstedt, T. J., and Immonen, I. J., "Early versus late staining of microaneurysms in fluorescein angiography", *Retina* vol.17, no.3, pp. 211–215, 1997.
[35] Bernardes, R., Nunes, S., Pereira, I., Torrent, T., Rosa, A., Coelho, D., and Cunha-Vaz, J., "Computer-assisted microaneurysm turnover in the early stages of diabetic retinopathy", *Ophthalmologica* vol. 223, no. 5, pp. 284–291, 2009.
[36] Jelinek, H. J., Cree, M. J., Worsley, D., Luckie, A., and Nixon, P., "An automated microaneurysm detector as a tool for identification of diabetic retinopathy in rural optometric practice", *Clin. Exp. Optom*. vol.89, no.5, pp. 299–305, 2006.
[37] Lee, S. C., Lee, E. T., Kingsley, R. M., Wang, Y., Russell, D., Klein, R., and Warn, A., "Comparison of diagnosis of early retinal lesions of diabetic retinopathy between a computer system and human experts", *Arch. Ophthalmol,* vol. 119, no. 4, pp .509–515, 2001.
[38] Niemeijer, M., van Ginneken, B., Russell, R. S., Suttorp -Schulten, S. A. M., and Abramoff, D. M ., "Automated detection and differentiation of drusen, exudates, and cotton-wool spots in digital color fundus photographs for diabetic retinopathy diagnosis", *Invest. Ophthalmol. Vis. Sci.* vol.48, no.5, pp. 2260–2267, 2007.
[39] Sopharak, A., Uyyanonvara, B., Barman, S., and Williamson, H. T., "Automatic detection of diabetic retinopathy exudates from non-dilated retinal images using mathematical morphology methods", *Comput. Med. Imaging Graph.* vol. 32, no. 8, pp. 720–727, 2008.
[40] "M icroaneurysms in diabetic retinopathy", *Br. Med. J.* 3(5774):548– 549, 1971.